NANO LETTERS

Letter

pubs.acs.org/NanoLett

Direct Imaging of Atomic-Scale Ripples in Few-Layer Graphene

Wei L. Wang,[†,‡] Sagar Bhandari,[‡] Wei Yi,[‡,∥] David C. Bell,[‡,§] Robert Westervelt,[†,‡] and Efthimios Kaxiras*[,†,‡]

[†]Department of Physics, [‡]School of Engineering and Applied Sciences, and [§]Center of Nanoscale Systems, Harvard University, Cambridge, Massachusetts 02138, United States

Supporting Information

ABSTRACT: Graphene has been touted as the prototypical two-dimensional solid of extraordinary stability and strength. However, its very existence relies on out-of-plane ripples as predicted by theory and confirmed by experiments. Evidence of the intrinsic ripples has been reported in the form of broadened diffraction spots in reciprocal space, in which all spatial information is lost. Here we show direct real-space images of the ripples in a few-layer graphene (FLG) membrane resolved at the atomic scale using monochromated aberration-corrected transmission electron microscopy (TEM). The thickness of FLG amplifies the weak local effects of the ripples, resulting in spatially varying TEM contrast that is unique up to inversion symmetry. We compare the characteristic TEM contrast with simulated images based on accurate first-principles calculations of the scattering potential. Our results characterize the ripples in real space and suggest that such features are likely common in ultrathin materials, even in the nanometer-thickness range.

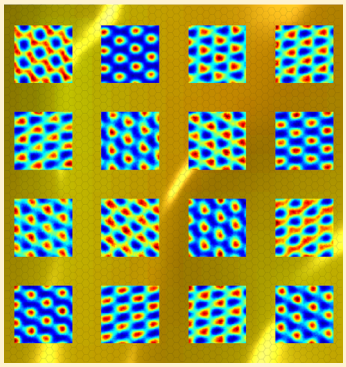

KEYWORDS: *Graphene ripples, aberration-corrected TEM, DFT, IAM*

The significance of the discovery of graphene[1,2] lies not only in its potential as a novel material for electronics[3] but more fundamentally in demonstrating that the ultimate limit of thinness in a material membrane is attainable. Prior to the realization of this single-atomic-layer of carbon, the thinnest material ever freely suspended over a gap had thickness in the range of tens of atomic layers, for example, a 15 nm nanocrystalline silicon film.[4] Theory predicted that in the limit of the ultimately thin material, a two-dimensional (2D) system cannot survive at finite temperature because thermal fluctuations would spontaneously destroy the long-range order of a 2D crystal.[5] Meyer et al.[2] showed that a free-standing single atomic layer of graphene does exist but in a nearly 2D form that has random elastic deformation in the third dimension,[2,6] as is indicated by the broadened spots in electron diffraction patterns. The broadening was attributed to atomic-scale ripples that had been described in a previous theory[7] as the result of coupling of the bending and stretching long-wavelength phonon modes.[8,9] The ripples appear to be an intrinsic property of thin membranes that affect their mechanical, electric and magnetic properties.[10−15] Despite these advances in understanding materials at the limit of thinness, there are still many unsolved issues. One issue of essential importance is what exactly the ripples look like in real space and whether or not they are static and permanent in nearly 2D systems.

Observation of the ripples is challenging because it requires both imaging at the atomic scale and detection of small deviations from flatness. Electron diffraction[2,6,16] is sensitive but cannot capture important spatial information, such as the precise size and amplitude of the ripples and whether or not the ripples are static. Convergent beam electron diffraction (CBED)[6] can detect certain local effects but is limited by spatial resolution and image interpretation. Although bond length variations in a high-resolution TEM image[17] can be related to the local tilt resulting from ripples, the detection sensitivity is rather low, corresponding to only a couple of pixels per bond for typical ripples. It is possible to observe the ripples in thicker samples[2] but only if the thickness does not suppress the ripples altogether. In this Letter, we show atomically resolved images of a free-standing few-layer graphene (FLG) membrane that exhibits aperiodic spatially varying patterns. In FLG samples, a small tilt of the local surface normal produces amplified change in the projected potential, that shifts the phase of passing electron waves and leads to changes in the image contrast. These local contrast patterns serve as fingerprints of the local tilt of the column of carbon atoms in the rippled crystalline thin film. We show through TEM image simulations that by varying the surface normal systematically, we are able to produce images that match the observed patterns and the obtained gradient field can be used to determine the topography of the ripples.

Our graphene samples are mechanically exfoliated[1] from natural graphene flakes, floated on water using a hydrophobic film[18] and then deposited on standard TEM grids (Figure 1a). The advantages of this method are that the area of interest in the sample can be aligned precisely on the open windows of the TEM grid and that the contamination from the scotch tape and the preparation processes are minimized. Raman spectra taken

Received: January 6, 2012
Revised: March 28, 2012
Published: April 2, 2012

   dx.doi.org/10.1021/nl300071y | *Nano Lett.* 2012, 12, 2278−2282

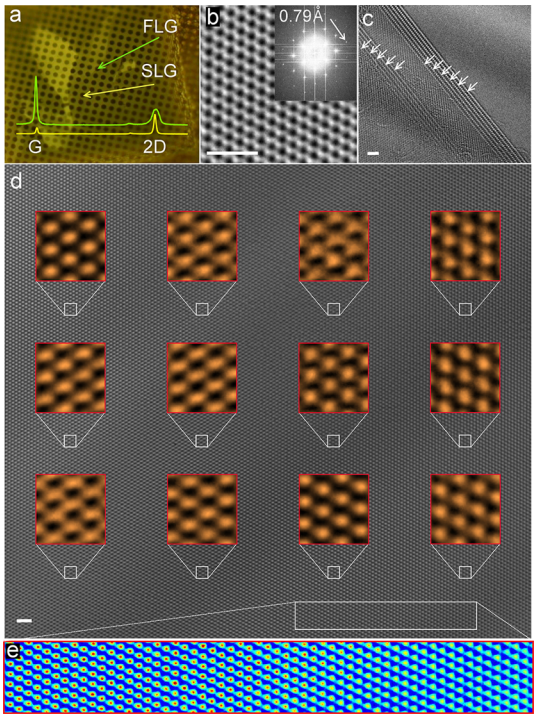

Figure 1. Sample preparation and direct TEM imaging of graphene membrane. All images are unfiltered. The scale bars in b–d are 1 nm. (a) Partially suspended graphene flakes across 1.2 μm holes of a standard TEM grid. Sample is examined with Raman spectroscopy and signatures for both SLG (red) and FLG (green) areas are identified, distinguished by the width and intensity ratio of the G and 2D peaks.[19] (b) TEM image of the FLG region. Fast Fourier transform of the image shown in the inset demonstrates a resolution better than 0.79 Å. (c) Fold at the edge of graphene membrane shows that the FLG area has 11 layers. (d) TEM images of the FLG sample. A 4 × 3 array of locally sampled images are enlarged and shown on top of the original image. The size of each inset image is 8 Å × 8 Å. (e) A selected area in the original TEM image is plotted with color, showing the gradually varying TEM contrast pattern, with dynamic range decreasing from left to right.

before and after the transfer process show identical signatures[19] in the identified single-layer and multiple-layer areas, excluding the possibility of mechanical damage or substantial contamination during the transfer.

We image the TEM samples with Libra 200 MC by Zeiss, a monochromated aberration-corrected TEM operated at 80 kV. The combination of objective-lens Cs correction and a FEG-source monochromator considerably improves the spatial and energy resolutions.[20] The electron beam from the field emission gun is energy filtered and passes through a selected 3.5 μm slit, which limits the energy spread of the beam to $\Delta E <$ 0.1 eV. The reduced spread of the beam energy expands the temporal coherence envelope function and increases the information limit. Figure 1b shows an image of a FLG, where the fast Fourier transform (inset) indicates that the information transfer is better than 0.79 Å, (which is well below the carbon–carbon bond length of 1.42 Å), yielding not only a clearly resolved graphene lattice but also the fine contrast details beyond the graphene lattice frequency. The achieved higher-frequency transfer is crucial because the variation of the fine details in the TEM contrast due to the ripples would otherwise not be observable.

Figure 1c shows the image of the edge of a selected FLG area. The fold at the edge reveals that the membrane has 11 layers. At a nominal magnification of 10^6, the sample appears defect-free and produces a high quality image across the entire scope, an area of 50 nm × 50 nm. The ripples result in significantly varying contrast patterns that gradually evolve spatially, as is shown in Figure 1d,e. In Figure 1d, superimposed on the original full scope image, we show TEM contrast patterns at a 4 × 3 array of sampled locations. At each sampled location, the local TEM contrast pattern is shown, unfiltered and enlarged by a factor of 8. Note that these contrast patterns are distinctly different from Moiré fringes or periodic buckling patterns observed in samples with lattice mismatch, typical in chemically processed FLG.[21,22] Those samples all exhibit in their TEM image periodicity larger than the primary cell of graphene, which originates from lattice mismatch and beating. Our FLG samples are minimally processed and free of interactions with harsh chemicals. The patterns we observe have exclusively the periodicity that corresponds to the primitive cell of graphene, but vary in appearance with location. The presence of the ripples is also supported by the observed gradual variation of dynamic range in the TEM contrast, as is shown in Figure 1e and Supporting Information Figure S1. The dynamic range decrease (increase) is a result of increased (decreased) deviation of the local normal from the TEM optical axis which makes the projected potential more (less) uniform. Our results can be compared to Figure 4 of ref 2 that showed spatial contrast variation in a multiple-layered graphene sample using TEM operated at 300 kV.[2] Our TEM was operated at 80 kV to avoid possible contrast variations contributed by sample damage at high beam energies and we have achieved high resolution that makes quantitative characterization in real space possible.

In order to understand these patterns and quantify the observations, it is necessary to conduct TEM image simulations and compare with the experimental data. In the simulations, it is important to reproduce accurately the projected total potential felt by the electrons as they pass through the specimen, which determines the image patterns. The total potential includes both single-particle terms and exchange-correlation effects. TEM images are routinely simulated using an approximation called independent atomic model (IAM).[23] This model superimposes single atomic potentials in the system and neglects all bonding effects, including the redistribution of electronic charge and the corresponding changes in the total potential. The difference may be insignificant in traditional TEM where substantial spherical aberration is present. However, for analyses based on aberration-corrected images, the error may lead to quantitatively or even qualitatively wrong results.[24] To account for bonding effects on the total potential, realistic first-principles methods based on, for example, density functional theory (DFT) must be used. Most efficient DFT codes utilize pseudopotentials and therefore yield wrong total potential in the core region. To remedy this issue, all-electron codes can be used[24] but for larger systems such as FLG the computational cost for all-electron calculations becomes prohibitive because of nearly exponential scaling.

We develop a strategy to efficiently calculate the accurate total potential of bonded systems in both the core and bonding regions by applying a transferable core correction to pseudopotential DFT results. In preparing the core-correction potential, we first obtain potentials for a single atom using DFT based on both all-electron and pseudopotential calculations. We

dx.doi.org/10.1021/nl300071y | Nano Lett. 2012, 12, 2278–2282

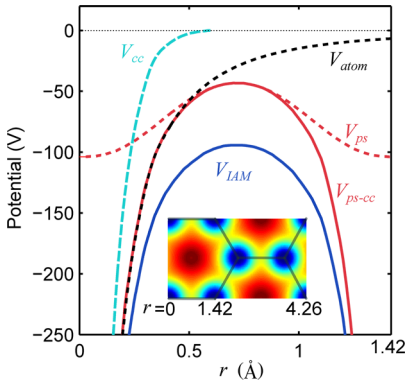

Figure 2. Total potential based on first-principles calculations. Construction of the DFT total potential and comparison to the potential based on IAM. Distance r is measured from one nucleus, and the plot is over a range corresponding to one bond length. The black dashed curve V_{atom} is the total potential of a single carbon atom obtained from all-electron calculations. The cyan curve V_{cc} is the core-correction potential with a cutoff at a core radius of r_0 = 0.6 Å . V_{IAM} (blue solid line) and V_{ps} (red dashed line) are the total potentials for graphene calculated based on IAM and pseudopotential DFT, respectively. The core-corrected total potential V_{ps-cc} (red solid line) based on pseudopotential DFT calculations retains the correct potential in the bonding region while it recovers the correct potential in the core region. The inset shows the potential difference between V_{ps-cc} and V_{IAM}, where blue is small and dark red is large and the total range is 50 V.

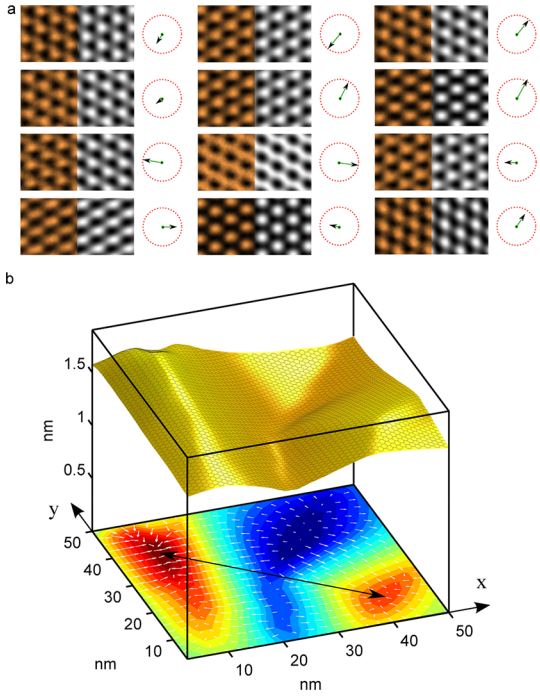

Figure 3. Image matching from experiment to simulations and reconstruction of the membrane topography. (a) Identified best matches for various patterns. On the left are the unfiltered TEM images, and on the right the simulated images. Next to each matched pair is the vector showing the local surface gradient, where the red dashed circle corresponds to a gradient amplitude of 0.12 (or tilt amplitude of 7°). (b) Gradient field and reconstructed topography of the rippled FLG surface. For the shown size of 50 × 50 nm area, the out-of-plane displacement is 0.5 nm with a standard deviation of 0.13 nm. The typical width of the ripple is 45 nm, as is indicated by the arrow in the contour plot. For easy visualization, the scale in vertical direction is amplified by a factor of 20 and the honeycomb lattice illustrated on the topography is enlarged by a factor of 4.

then subtract the pseudopotential part from the all-electron potential. The resultant core potential correction V_{cc}, shown in Figure 2, has a short cutoff at 0.6 Å for carbon. Assuming the core potential is largely unaffected during bonding, this core correction is generally transferable and can be applied to the total potential V_{ps} obtained by the efficient calculations based on pseudopotentials. In bonded systems, the total potential V_{ps-cc} based on pseudopotential DFT with the core correction (psDFT-cc) reproduces well the correct potential in both the core and bonding regions. On the other hand, it is clear that the IAM potential V_{IAM}, is substantially different in amplitude. This is expected because for an independent atom the potential is screened over a long distance while in the bonded system the screening of the core potential by the valence electrons is much more effective. The difference contributes not only to an underestimated background but also to the difference in the projected potential and thus in the TEM image contrast, particularly as the information transfer improves (see Supporting Information Figure S2). In our study of the ripples in FLG, we manage to minimize the beam energy spread and spherical aberration to retain higher-frequency transfer for the fine details in the image contrast, therefore, it is essential to employ an accurate potentials for the image simulation.

Once the total potential of the FLG system is obtained, it is projected along the given local tilt directions and used in the subsequent TEM image simulations. Indeed, by systematically varying the tilt angle, experimentally observed atomic-scale pattern variations are readily reproduced. Figure 3a shows for various patterns the comparison between the experimental TEM images and the matched images (tilt angle) from the simulations. The local gradient $\vec{\nabla}h = \partial h/\partial x\ \hat{x} + \partial h/\partial y\ \hat{y}$ corresponding to the matched tilt angle is given, where h is the membrane surface height. From the experimental TEM image, we selected a 20 × 20 array of local images, which is then compared to a systematically generated library of simulated images. The normalized cross-correlation C is computed for each comparison to identify the best matching (see Methods). Since the projected potential of the carbon atom columns has a C_2 symmetry, the best matching is only determined up to inversion symmetry with respect to the inclination angle, as is illustrated in Supporting Information Figure S3. An additional restriction of continuity can be applied to uniquely determine the entire gradient field up to global inversion symmetry. It is important to clarify that the reconstruction takes into account the dominating effect of the local tilt while higher order effects such as stress and slide between layers are neglected because here the amplitude of the ripples are expected small compared to their lateral sizes.

The gradient field obtained can then be used to reconstruct the topography of the graphene membrane, as is shown in Figure 3b. We utilize a Fourier transform based nonlocal algorithm that is robust against local noise.[25] The reconstructed surface is checked for self-consistent integrability (Supporting Information Figure S4), which is accurate within the given resolution of matching. In the contour plot (Figure 3b), we identify a characteristic wavelength of 45 nm and a maximum height deviation of 0.5 nm for the given area of 50 × 50 nm, which is in an order-of-magnitude agreement with a previous study using electron diffraction,[2] where the spatial information is not directly available and the amplitude was estimated to be 1

dx.doi.org/10.1021/nl300071y | Nano Lett. 2012, 12, 2278−2282

nm based on the coherence length, the illuminated area size, and the local normal tilt angles. Previous simulations[9] on single layer graphene gave a wavelength ~8 nm at 300 K, six times smaller than in our sample, which is ten times thicker. This is consistent with the trend that for a thicker membrane with larger bending stiffness one expects the anharmonic coupling to take effect at a larger wavelength, thereby shifting the peak in the correlation function of the normals to lower frequencies. The same simulation[9] yielded a ripple amplitude of 0.7 Å at 300 K, which is an order of magnitude smaller than what is reported in most experiments. According to the predictions of the phenomenological model on flexible membranes, the mean-square displacement in the direction normal to the layer is $\langle h^2 \rangle \propto TL^2/\kappa$ where L is the linear size of the sample and κ is the bending rigidity. The temperature T here is not precisely known. In our high-resolution TEM imaging, high brightness is required and the electron beam flux in the illuminated area on the sample is high, on the order of 1 pA/nm^2. It is possible that electron irradiation raises the temperature in the imaged area and contributes to the larger amplitude of the ripples, compared to the value at room temperature conditions or in the TEM diffraction mode. Finally, our real-space observation shows that the ripples are static, at least on the 10 s time scale that the image is taken. Otherwise, the spatially varying fingerprints of the ripples we observed would have been smeared or averaged out.

Our results reveal the spatial characteristics of the atomic-scale ripples, a fundamentally new phenomenon that is likely common for ultrathin materials in the 2D and nearly-2D range. Even when the membrane is supported on a substrate, the ripples are not entirely suppressed and are bound to affect the properties of the ultrathin material considerably.[10−15] Besides graphene, a family of single atomic layer materials such as BN, MoS_2, and $Bi_2Sr_2CaCu_2O_x$ have been identified in experiment,[16,26] although it is not yet clear if all would survive suspension because bonding topology and strength might affect the stabilization mechanism of the ripples. From single atomic layer to few layers and to the nanometer thickness range, there are numerous possibilities of forming layered and nonlayered ultrathin systems of novel composition. It would be interesting to investigate the presence of ripples in such systems and how they affect the structural stability and functional properties.

Methods. *Preparation of Suspended Graphene Membrane Sample for TEM Imaging.* The graphene sample is obtained from natural graphite flakes (Asbury Carbons Co.) that are subjected to repeated mechanical exfoliation with low contamination SEC blue tape (Loomis Industries) and pressed on a silicon wafer with 285 nm thick layer of oxide. A thin layer of hydrophobic polymer cellulose acetate butyrate[18] (30 mg/mL in ethyl acetate) is spun on top of the silicon wafer with the graphene sample at 1000 rpm for 30 s. The polymer film is then wedging floated on water together with the graphene sample. The hydrophobic film is aligned under an optical microscope and deposited on the TEM grid (Quantifoil) before being washed away with acetone, leaving the graphene membrane suspended on the TEM grid.

Imaging the Graphene Membrane with TEM. The suspended graphene sample is imaged with Libra 200MC TEM from Carl Zeiss, a monochromated, aberration-corrected TEM equipped with a field emission gun (80−200 kV) and an in-column energy filter. The aberration correction is applied with the CETCOR software interface (CEOS GmbH, Heidelberg, Germany) up to third order. The spherical aberration is set at 5 μm and a defocus of 5 nm (Scherzer defocus) is used. All image data reported in this paper were based on the same aberration correction parameters unless otherwise specified.

First-Principles Calculations and TEM Image Simulation. The total potentials of the FLG system and the carbon atom are calculated using the density functional theory (DFT) method with normconserving pseudopotentials[27] as implemented in the SIESTA code.[28] The geometries of the FLG system were optimized using the conjugate gradient algorithm and a 0.04 eV/Å maximum force convergence criterion. The atomic potential of carbon is also calculated with the all-electron code ATOM, for the core correction term. In all cases, the generalized gradient approximation (GGA) exchange-correlation density functional PBE[29] was employed together with a double-ζ plus polarization basis set and a mesh cutoff of 200 Ry. The total potential of the FLG system after core-potential correction is projected according to given tilt directions. TEM simulations are carried out based on the projected potential, and the calculations of electron waves and TEM images follow the procedures described for a thin specimen as in Chapter 3 of ref 20.

Image Matching and Topography Reconstruction. Image matching is implemented by calculating the cross-correlation of the experimental TEM images and the simulated images. A normalized cross-correlation functional[23] C is computed in the search for the best match

$$C(f_{\mathrm{exp}}, f_{\mathrm{sim}}) = \frac{\sum_{xy} (f_{\mathrm{exp}}(x,y) - \bar{f}_{\mathrm{exp}})(f_{\mathrm{sim}}(x,y) - \bar{f}_{\mathrm{sim}})}{\sqrt{\sum_{xy} (f_{\mathrm{exp}}(x,y) - \bar{f}_{\mathrm{exp}})^2 \sum_{xy} (f_{\mathrm{sim}}(x,y) - \bar{f}_{\mathrm{sim}})^2}} \quad (1)$$

where $f(x,y)$ is the local pixel intensity and $\bar{f}$ is the global intensity average. Each local contrast pattern from the TEM experiment is compared to all the simulated images based on the array of tilt angles. The best matches are founded and the corresponding local inclinations yield the overall gradient field. Reconstruction of the topology from the gradient field is based on a nonlocal Fourier transform algorithm.[25] The reconstruction is coded as a self-consistent process where the input gradient field is compared to the gradient field computed for the reconstructed surface. The difference contributes with a weight to the fine-tuning of the initial tilt angle matching.

■ ASSOCIATED CONTENT

Supporting Information

Description of the material. This material is available free of charge via the Internet at http://pubs.acs.org.

■ AUTHOR INFORMATION

Corresponding Author

*E-mail: kaxiras@physics.harvard.edu.

Present Address

[‖]Hewlett-Packard Laboratories, Palo Alto, California 94304, USA.

Notes

The authors declare no competing financial interest.

■ ACKNOWLEDGMENTS

This work is partially supported by the Department of Energy Grant DE-FG02-07ER46422.

REFERENCES

(1) Novoselov, K. S.; et al. Electric field effect in atomically thin carbon films. *Science* **2004**, *306*, 666−669.
(2) Meyer, J. C.; et al. The structure of suspended graphene sheets. *Nature* **2007**, *446*, 60−63.
(3) Geim, A. K.; Novoselov, K. S. The rise of graphene. *Nat. Mater.* **2007**, *6*, 183−191.
(4) Striemer, C. C.; Gaborski, T. R.; McGrath, J. L.; Fauchet, P. M. Charge- and size-based separation of macromolecules using ultrathin silicon membranes. *Nature* **2007**, *445*, 749−753.
(5) Mermin, N. D. Crystalline order in two dimensions. *Phys. Rev.* **1968**, *176*, 250−254.
(6) Meyer, J. C.; et al. On the roughness of single- and bi-layer graphene membranes. *Solid State Commun.* **2007**, *143*, 101−109.
(7) Nelson, D. R.; Peliti, L. Fluctuations in membranes with crystalline and hexatic order. *J. Phys. (Paris)* **1987**, *48*, 1085−1092.
(8) Nelson, D. R.; Piran, T.; Weinberg, S. Statistical mechanics of membranes and surfaces, 2nd ed.; World Scientific Pub.: New York, 2004.
(9) Fasolino, A.; Los, J. H.; Katsnelson, M. I. Intrinsic ripples in graphene. *Nat. Mater.* **2007**, *6*, 858−861.
(10) de Juan, F.; Cortijo, A.; Vozmediano, M. A. H. Charge inhomogeneities due to smooth ripples in graphene sheets. *Phys. Rev. B* **2007**, *76*, 165409.
(11) Herbut, I. F.; Juricic, V.; Vafek, O. Coulomb interaction, ripples, and the minimal conductivity of graphene. *Phys. Rev. Lett.* **2008**, *100*, 046403.
(12) Guinea, F.; Horovitz, B.; Le Doussal, P. Gauge field induced by ripples in graphene. *Phys. Rev. B* **2008**, *77*, 205421.
(13) Guinea, F.; Horovitz, B.; Le Doussal, P. Gauge fields, ripples and wrinkles in graphene layers. *Solid State Commun.* **2009**, *149*, 1140−1143.
(14) Miranda, R.; de Parga, A. L. V. Graphene Surfing ripples towards new devices. *Nat. Nanotechnol.* **2009**, *4*, 549−550.
(15) Guinea, F.; Katsnelson, M. I.; Geim, A. K. Energy gaps and a zero-field quantum Hall effect in graphene by strain engineering. *Nat. Phys.* **2010**, *6*, 30−33.
(16) Brivio, J.; Alexander, D.; Kis, A. Ripples and layers in ultrathin MoS_2 membranes. *Nano Lett.* **2011**, *11* (12), 5148−5153.
(17) Bangert, U.; Gass, M. H.; Bleloch, A. L.; Nair, R. R.; Geim, A. K. Manifestation of ripples in free-standing graphene in lattice images obtained in an aberration-corrected scanning transmission electron microscope. *Phys. Status Solidi A* **2009**, *206*, 1117−1122.
(18) Schneider, G. F.; Calado, V. E.; Zandbergen, H.; Vandersypen, L. M. K.; Dekker, C. Wedging transfer of nanostructures. *Nano Lett.* **2010**, *10*, 1912−1916.
(19) Ferrari, A. C.; et al. Raman spectrum of graphene and graphene layers. *Phys. Rev. Lett.* **2006**, *97*, 4.
(20) Bell, D. C.; Russo, C. J.; Benner, G. Sub-Angstrom low-voltage performance of a monochromated, aberration-corrected transmission electron microscope. *Microsc. Microanal.* **2010**, *16*, 386−392.
(21) Singh, M. K.; et al. Atomic-scale observation of rotational misorientation in suspended few-layer graphene sheets. *Nanoscale* **2010**, *2*, 700−708.
(22) Mao, Y. D.; Wang, W. L.; Wei, D. G.; Kaxiras, E.; Sodroski, J. G. Graphene structures at an extreme degree of buckling. *ACS Nano* **2011**, *5*, 1395−1400.
(23) Kirkland, E. J. Advanced computing in electron microscopy; Springer: New York, 2010.
(24) Meyer, J. C.; et al. Experimental analysis of charge redistribution due to chemical bonding by high-resolution transmission electron microscopy. *Nat. Mater.* **2011**, *10*, 209−215.
(25) Wei, T. G.; Klette, R. Depth recovery from noisy gradient vector fields using regularization; *Computer Analysis of Images and Patterns: 10th International Conference, CAIP 2003, Groningen, The Netherlands, August 25-27, 2003, Proceedings (Lecture Notes in Computer Science)* Springer, 2003, *2756*, 116−123.
(26) Novoselov, K. S.; et al. Two-dimensional atomic crystals. *Proc. Natl. Acad. Sci. U.S.A.* **2005**, *102*, 10451−10453.
(27) Kresse, G.; Joubert, D. From ultrasoft pseudopotentials to the projector augmented-wave method. *Phys. Rev. B* **1999**, *59*, 1758−1775.
(28) Soler, J. M.; et al. The SIESTA method for ab initio order-N materials simulation. *J. Phys.: Condens. Matter* **2002**, *14*, 2745−2779.
(29) Perdew, J. P.; Burke, K.; Ernzerhof, M. Generalized gradient approximation made simple. *Phys. Rev. Lett.* **1996**, *77*, 3865−3868.